Journal of Alloys and Compounds 509 (2011) 6935–6941

Contents lists available at ScienceDirect

Journal of Alloys and Compounds

journal homepage: www.elsevier.com/locate/jallcom

Glucose-mediated solution–solid route for easy synthesis of Ag/ZnO particles with superior photocatalytic activity and photostability

Chungui Tian, Qi Zhang, Baojiang Jiang, Guohui Tian, Honggang Fu*

Key Laboratory of Functional Inorganic Material Chemistry, Ministry of Education of the People's Republic of China, Heilongjiang University, Harbin 150080, PR China

ARTICLE INFO

Article history:
Received 20 December 2010
Received in revised form 30 March 2011
Accepted 1 April 2011
Available online 7 April 2011

Keywords:
ZnO
Silver
Photocatalysis
Photostability

ABSTRACT

In this paper, we report an effective glucose-assisted solution–solid process for preparing Ag/ZnO photocatalyst with excellent photocatalytic performance. The solution–solid route included first formation of a glucose–Zn–Ag precursor containing Zn and Ag source in glucose framework (solution-phase stage) and subsequent heat treatment of the precursor to obtain Ag/ZnO particles (solid-phase stage). Ag/ZnO particles could be prepared on large scale through this solution–solid process (about 1.5 g for each time synthesis and could be easily scaled up). Also, the result of photocatalytic test indicates that the material exhibits superior photocatalytic activity for the photodegradation of organic dye Rhodamine B. Notably, no obvious loss of catalytic activity was observed after ten cycles, indicating the excellent photostability of Ag/ZnO particles.

1. Introduction

With industrialization and social development, environmental pollution caused by organic pollutants becomes one of the most important problems faced by all worlds. Most dyes are toxic, long-lived, and highly resistant against degradation. Photocatalysis has received intensive attention because of its potential ability for eliminating the pollution in water and air while without causing additive damage to our environment [1–4]. Under light irradiation, contaminations could be decomposed into non-toxic substance on the surface of photocatalyst. A suitable photocatalyst should be stable, nontoxic, and able to utilize light with a high efficiency. Since the pioneering work by Fujishima and Honda in 1972 [5], enormous attention has been devoted to the use of TiO_2 as photocatalyst due to its relatively high efficiency, low cost, and nontoxic nature [6]. Recently, ZnO, a wide bandgap semiconductor, has been considered as a promising alternative to TiO_2 due to its nontoxic characteristics and lower preparation cost than TiO_2 [7,8]. In fact, ZnO has been a close competitor of TiO_2 historically [9]. Hoffman et al. have observed the production of H_2O_2 on ZnO surface as early as 1994 [10]. However, the application of ZnO as photocatalyst has been limited due to its low photocatalytic activity and photocorrosion that can lead to a severe decrease in activity of ZnO photocalysts in reuse process [11]. The development of nanotechnology provides an opportunity for tuning of the photocatalytic performance of nanomaterials based on their morphology-related properties. Ramakrishna and Ghosh have reported that the photocatalytic activity decreased with the increase of the particle size of ZnO [12]. Kaneva et al. have demonstrated the dependence of photocatalytic activity on the preparative procedure of ZnO films [13]. Also, some researchers found the face- and morphology-dependent photocatalytic performance of ZnO crystals [14–17]. Generally, the $(0\,0\,0\,1)$ and $(0\,\,0\,\,0\,\,\bar{1})$ facets of the hexagonal ZnO crystals can exhibit specific activity for photodegradation of organic contaminations. Recently, it was found that the hierarchical ZnO microarchitectures assembled by ultrathin nanosheets exhibited enhanced photocatalytic activity due to the presence of high proportion of active $(0\,0\,0\,1)$ planes in the structure [18]. Nevertheless, the activity of most of these ZnO materials is usually not as high as TiO_2, especially Degussa P25, a benchmark photocatalyst. Lu et al. [19] have found that the high BET is helpful for improving the photocatalytic activity. In the study, ZnO hierarchical micro/nano-architecture, which was obtained in EDA–water mixed solvent, exhibited better performance than Degussa P25 TiO_2, contributing to its high specific surface area ($185.6\,m^2/g$) and special hierarchical structure. However, the efficiency had obviously decreased from 100% of first use to about 93% of three reuses, attributed to photocorrosion under experimental condition [19].

An effective strategy allowing to increase the activity of ZnO is to combine it with noble metal nanoparticles, such as Au, Ag, Pt, and Pd. These noble metals are well-known advanced materials in the fields of biomedical diagnostics, catalysis, optical devices, and data storage [20]. As known, the electronic structure of semiconductor is characterized by a valence band (VB) filled with electrons and an

* Corresponding author. Fax: +86 451 86608458.
E-mail address: fuhg@vip.sina.com (H. Fu).

0925-8388/$ – see front matter © 2011 Elsevier B.V. All rights reserved.
doi:10.1016/j.jallcom.2011.04.005

empty conduction band (CB). The metal NPs can be described as a charge sink [21]. Under irradiation, the electrons promoted from VB to CB of semiconductor will be captured by the metal NPs, prohibiting the recombination of photo-generated carriers and thus improving the photoelectrochemical performance of the semiconductor particles [22]. It was demonstrated that Pt/ZnO and Au/ZnO exhibited enhanced photocatalytic activity [23–29]. However, the high price of Pt and Au is a concern for widespread industrial use. Ag is the cheapest noble metal, which should be favorable for the practical use of Ag-based materials. Some attempts to Ag/ZnO photocatalyst have been done [30–37]. Generally, Ag NPs could be deposited on the surface of preformed semiconductor particles upon UV-light irradiation [30,31]. Gu's group prepared ZnO@Ag heterostructures by depositing ZnO on the surface of pre-synthesized Ag nanowires [32]. Other strategies, such as co-precipitation process, solvothermal route, electrospun, template methods and sonochemical method were also useful to synthesize this kind of materials [33–36]. Zhang et al. reported the preparation of Ag–ZnO nanosheet composites, in that the silver nanoparticles grow on the surface of ZnO sheets, through a "liquid–liquid" two-phase method [37]. It is shown that the photocatalytic performance of ZnO could be greatly enhanced by introducing Ag NPs. In a few studies about reuse test, it was found that the photostability of ZnO could be improved by Ag NPs modification [35]. Nevertheless, most synthesis is based on a solution-phase process. The formation of Ag/ZnO occurs usually in the solution environment, where reagents with low-concentration are used, thus leading to a low output of the resulting catalyst. Some solid-based processes, for example electrospun, have usually suffered from complicated handling and time-consuming. Therefore, a facile method for large-scale synthesis of Ag/ZnO photocatalysts with a good activity and stability still remains a key challenge.

Recently, we reported the preparation of Ag/ZnO microsphere composites through a one-pot reaction in ethylene glycol medium, and found an enhanced photocatalyst activity and stability of the composites compared to that of pure ZnO [38]. In this paper, we reports a more facile and economical route, namely glucose-assisted solution–solid process, for large-scaled preparation of Ag/ZnO photocatalyst that has shown an excellent photocatalytic activity and reuse performance for dye photodegradation. The selection of glucose was based on its following characteristics, that is, it can coordinate with metal ions and easily polymerize under lower temperature [39], which provides a chance to incorporate desirable precursors into the "polymeric" glucose framework. Our synthesis could be described as a "solution–solid" process. Specifically, the glucose–Zn–Ag precursor composed of Zn and Ag source in polymeric glucose framework formed firstly through a solution-phase process. After solid-phase heat treatment, ZnO and Ag phases formed due to the interaction of glucose unit with Zn and Ag component in the precursor [40]. In the preparation of the precursor, the reagent (Zn and Ag salts) could be used with a high concentration. At the same time, the subsequent solid-based reaction has less limitation in concentration. Therefore, Ag/ZnO particles could be obtained with a high yield (about 1.5 g for each time synthesis and can be easily scaled). Notably, the photocatalytic test indicated that Ag/ZnO particles exhibited superior photocatalytic activity for photodegradation of Rhodamine B dye. After ten cycles, the catalyst had not obvious loss of photocatalytic activity, demonstrating the excellent reuse performance of Ag/ZnO catalyst.

2. Experimental

2.1. Synthesis

All chemicals used were of analytical grade and were used as received without further purification. In a typical synthesis, 0.03 mol of glucose, 0.02 mol $Zn(Ac)_2{\cdot}2H_2O$ and 0.001 mol $AgNO_3$ were dissolved in 10 mL H_2O successively. During heating on a magnetic stirring and heating apparatus at 90–100 °C under stirring, the solution gradually became sticky and finally formed a "solid" (solution-phase stage). The solid was placed a crucible and then calcinated in a muffle furnace (SX2-4-10, Tianjin Huabei Experimental Instruments Co., Ltd.) from room temperature to final temperature (600 °C) with a heating rate of 5 °C min^{-1} in an air atmosphere and kept at the maximum temperature for 120 min (solid-phase stage). The sample was denoted as 5%-Ag/ZnO, where 5% refers to the molar ratio of Ag–ZnO calculated on the basis of the initial amount of Zn and Ag salts. 2.5%-Ag/ZnO and 10%-Ag/ZnO samples were also prepared following the same procedure. The pure ZnO was also fabricated through the same process except no addition of the $AgNO_3$.

2.2. Characterization

Transmission electron microscopy (TEM, JEOL-2010) with an acceleration voltage of 200 kV was used to characterize the morphology of samples. X-ray powder diffraction (XRD) was performed with a Rigaku (Japan) D/MAX-rA X-ray diffractionmeter equipped with graphite monochromatized Cu Kα radiation (γ = 1.541874 Å). X-ray photoelectron spectroscopy (XPS) analysis was performed on a VG ESCALAB MK II with a Mg Kα (1253.6 eV) achromatic X-ray source. Fourier transform infrared (FT-IR) spectra were carried out on NICOLETiS10 FT-IR spectrometer. The nitrogen adsorption/desorption isotherms were measured at 77 K using a Micromeritics Tristar II. Before measurement, the samples were out gassed at 150 °C for 4.5 h; the specific surface area of the materials was calculated by the Brunauer–Emmett–Teller (BET) theory.

2.3. Photocatalytic test

The photocatalytic performance of the Ag/ZnO samples was evaluated by using Rhodamine B (RhB) dye as a representative pollutant. In detail, 0.04 g catalyst (Ag/ZnO, Degussa P25 and ZnO) and 40 mL of 10 mg/L RhB aqueous solution was mixed in a 100 mL reaction cylinder under ultrasound. After stirring in the dark for 30 min to reach the adsorption equilibrium, the suspension was irradiated with 15-W UV light-tube (365 nm) for a given time under continuous magnetic stirring. A UV-2550 spectrometer was used to measure the concentration of RhB. The parameters in recycled experiments are the same as those in the first testing, with the exception that the catalyst was recollected by centrifugation at 3500 rpm/min.

3. Results and discussion

3.1. Structure characterization of Ag/ZnO samples

The Ag/ZnO samples are synthesized through a solution–solid process with a high yield. The synthetic procedure is illustrated in Scheme 1. The structure and composition of the samples are investigated by XRD, XPS and TEM techniques. Fig. 1 shows the XRD

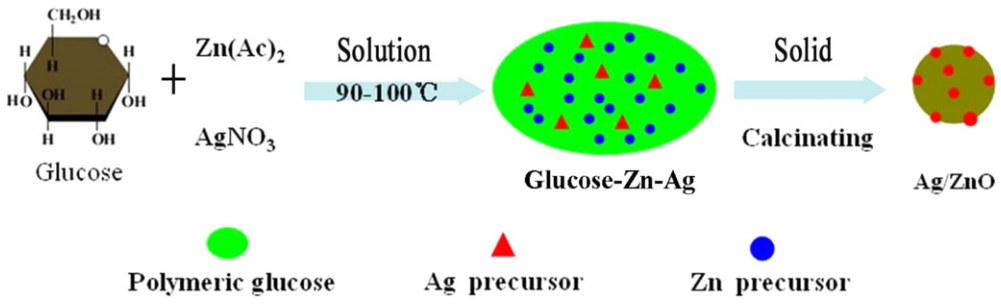

Scheme 1. Schematic procedure for the fabrication of Ag/ZnO particles.

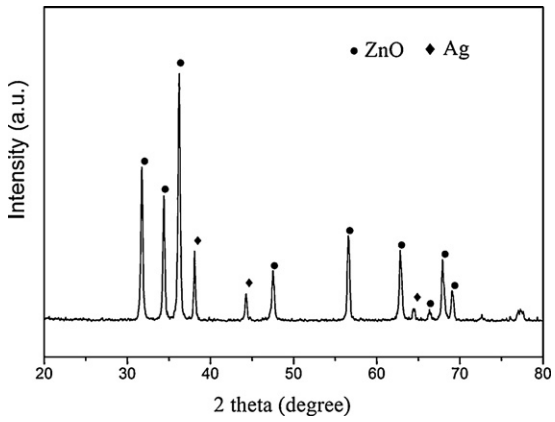

Fig. 1. XRD pattern of 5%-Ag/ZnO particles.

pattern of a typical sample, 5%-Ag/ZnO. As shown, the diffraction peaks at $2\theta = 31.7^\circ$, 34.4°, and 36.2° are indexed to (1 0 0), (0 0 2) and (1 0 1) diffractions of hexagonal structured ZnO (wurtzite), respectively (JCPDS no. 36-1451). The peaks located at $2\theta = 38.2^\circ$ and 44.4° are characteristic to (1 1 1) and (2 0 0) diffractions of face-centered-cubic structured Ag (JCPDS no. 04-0783). XRD test shows the presence of ZnO and Ag phases in the samples. XPS spectra of the sample are shown in Fig. 2. Several obvious peaks of Zn, O, and Ag elements were observed. Also, the high resolution XPS in Fig. 2b indicates that the Ag 3d5/2 peak located at 367 eV experiences a significant shift (1.2 eV) with respect to that of bulk metal Ag (368.2 eV), attributed to the electron transformation from Ag to ZnO [35]. In addition, the O 1s peak can be divided into two peaks at about 530 and 531.8 eV (Fig. 2c), corresponding to the lattice oxygen and surface hydroxyl oxygen, respectively. The TEM image (Fig. 3a) shows that small dots (Ag particles) are located on the surface of ZnO particles with size in the range of 50–100 nm. HRTEM image (Fig. 3b) clearly indicates that the Ag NPs with a size about 10 nm contact intimately with the ZnO particles. In addition, free Ag nanoparticles are also observed. The particle sizes were calculated by the Scherrer equation based on XRD results. The average crystallite size of ZnO is about 56 nm that is in the range observed by TEM. The grain size of Ag is about 18 nm that is slightly larger than those from TEM observation. This may be due to that the sample was treated at higher temperature, thus the crystalline of Ag was greatly improved, resulting positive error of particle size between Scherrer equation and TEM observation. As control, ZnO particles were prepared according to the same procedure, except with no use of Ag precursor in the preparation. From TEM images, one can see the particles with a smooth surface (Fig. 3c and d). The above results indicate that Ag/ZnO particles are successfully fabricated by the glucose-assisted solution–solid process. In addition, 2.5%-Ag/ZnO and 10%-Ag/ZnO samples were also fabricated followed a same procedure by tuning the ratio of Ag salts and zinc salts. XRD patterns of ZnO, 2.5 wt%-Ag/ZnO and 10 wt%-Ag/ZnO samples are given in Fig. S1. As shown, the relative peak intensity of Ag phase gradually increases with the increase of Ag/ZnO ratio, indicating the increase of Ag content in the sample. The size of Ag particle calculated by the Scherrer formula is about 15 and 32 nm for 2.5%-Ag/ZnO and 10%-Ag/ZnO samples, respectively. Compared with that for 5% Ag/ZnO, the size of Ag particles has no obviously change for 2.5%-Ag/ZnO sample, but it has an increase for 10%-Ag/ZnO sample. In addition, the particle size of ZnO in different samples has no obvious change (50, 55, and 52 nm for ZnO, 2.5 wt%-Ag/ZnO, and 10 wt%-Ag/ZnO, respectively) based on XRD analysis. This should be due to the invariable amount of Zn precursor used in our synthesis.

The formation process of Ag/ZnO particles is primarily investigated with an assistance of XRD and IR technique. The reaction rate is too fast to capture the composition change as calcination is performed at 600 °C, while it is relatively slow at low temperature. Therefore, the composition change is studied by temperate-dependent experiments. A black solid is obtained when the calcination is performed at 200 °C for 2 h (the sample is denoted as S-200). The XRD pattern in Fig. 4a indicates the emergence of Ag phase in the products, and no ZnO phase is observed. With increasing the temperature to 300 °C (S-300), three new peaks,

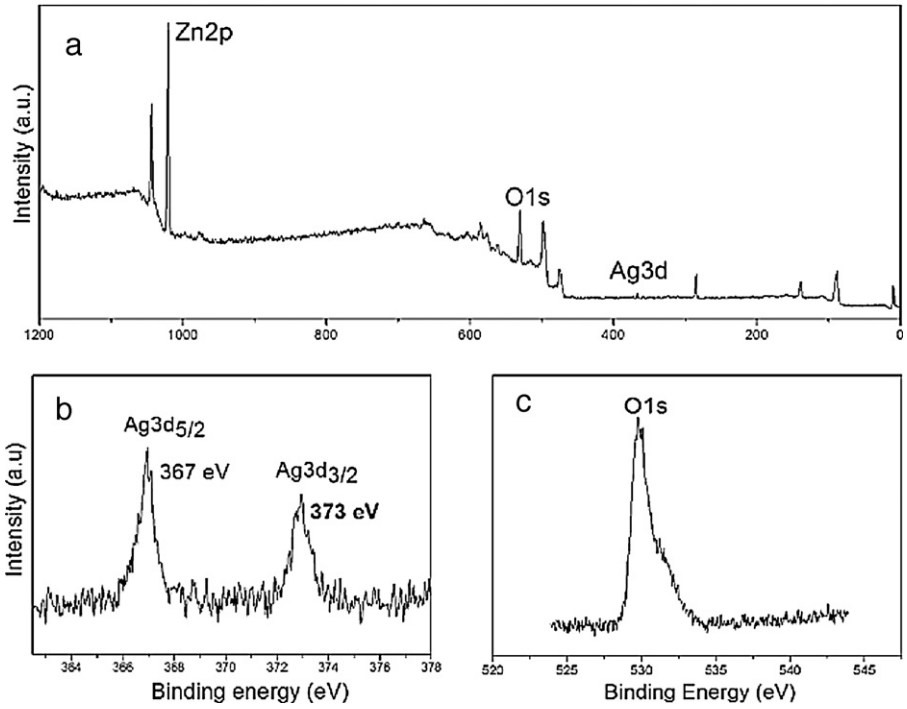

Fig. 2. (a) XPS spectrum of 5%-Ag/ZnO particles and the high-resolution spectra of (b) Ag 3d and (c) O 1s.

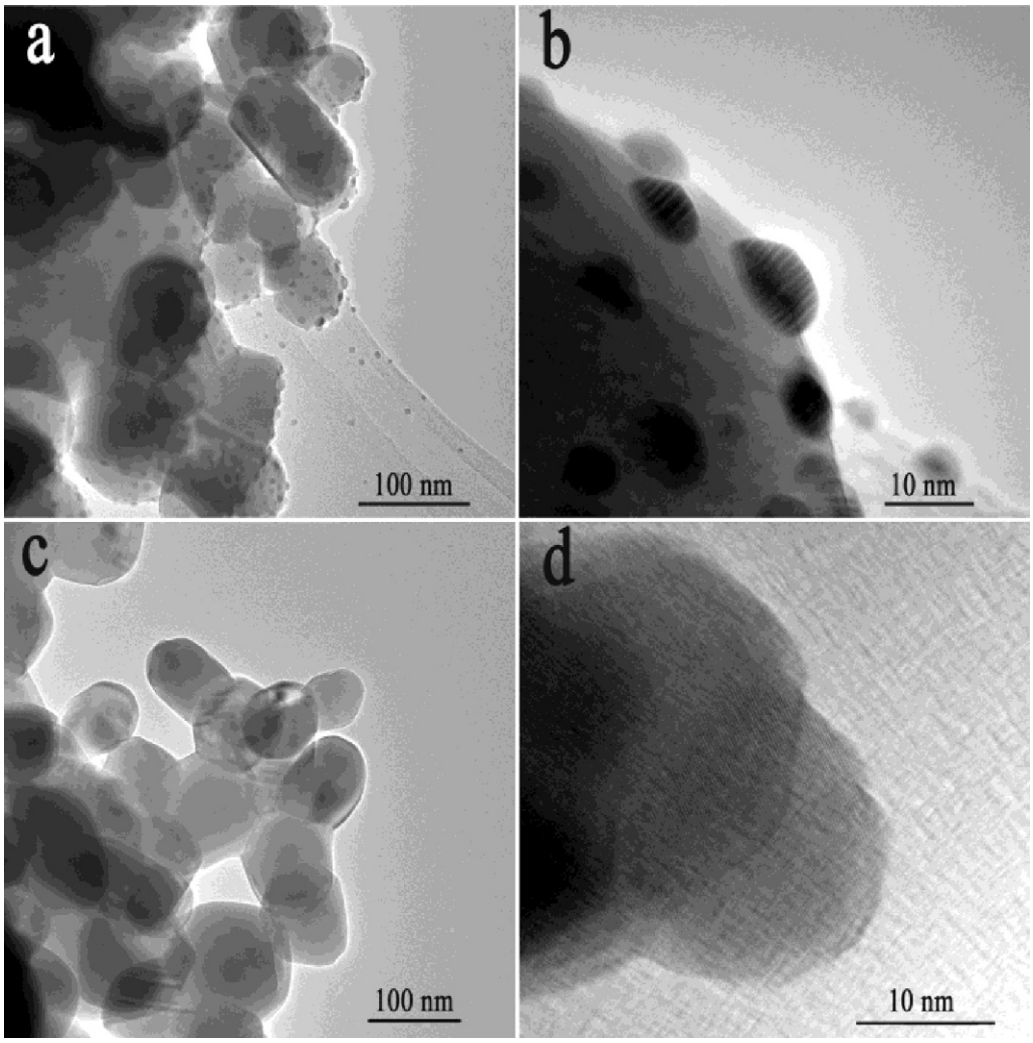

Fig. 3. (a) TEM images of 5%-Ag/ZnO (a and b) and pure ZnO samples (c and d).

contributing to (1 0 0), (0 0 2), and (1 0 1) diffractions of hexagonal structured ZnO (wurtzite) are observed (Fig. 4b). The peaks of ZnO phase become stronger and sharper for sample S-400 compared to that for sample S-300 (Fig. 4c). This indicates the improvement in crystalline order of the ZnO phase. Also, one can see a further increase in the peak intensity ratio of ZnO phase to Ag phase as the temperature increases from 400 °C to 500 °C (Fig. 4d). In addition to XRD that give an information about the phase change, IR spectra provide an information about the evolution of the functional group during the heat treatment (Fig. 5). The IR spectra of sample S-200 show several obvious peaks in the range of 1000–1700 $^{-1}$ cm^{-1}, around the 2900 cm^{-1} and 3400 cm^{-1}, contributing to the vibration of organic group in the glucose unit (Fig. 5a). Peak intensity of these organic groups becomes weak with the increase of heat tem-

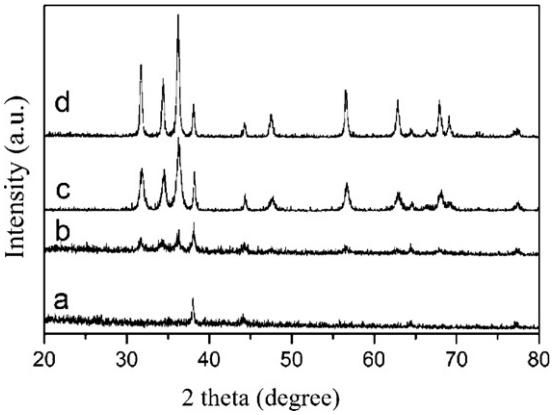

Fig. 4. XRD patterns of the products obtained by calcinating the precursor at 200 °C (a) 300 °C (b) 400 °C (c) and 500 °C (d) for 2 h.

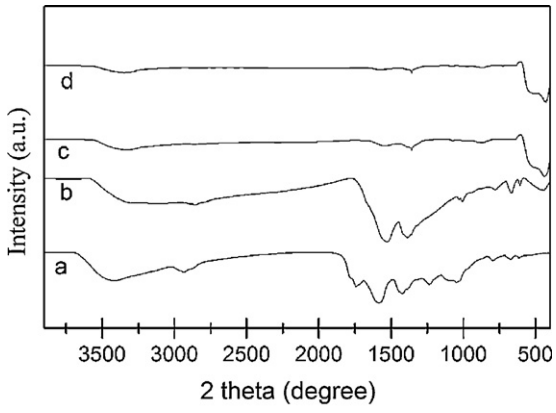

Fig. 5. IR spectra of the products obtained by calcinating the precursor at 200 °C (a), 300 °C (b), 400 °C (c) and 500 °C (d) for 2 h.

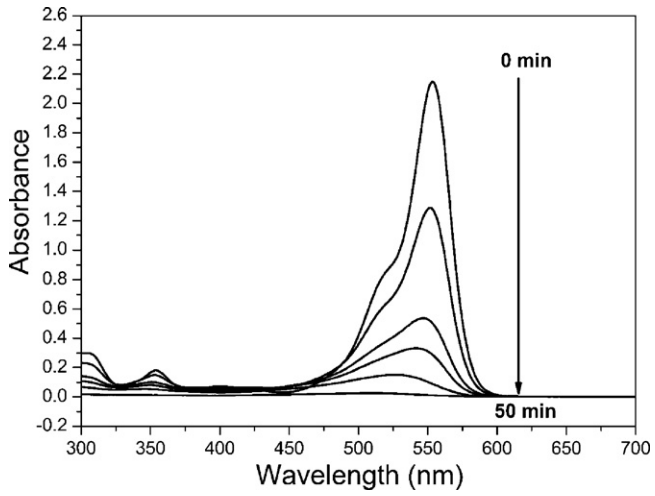

Fig. 6. UV–vis absorption spectra of RhB solution after irradiation with UV light for different time in the presence of Ag–ZnO photocatalyst. The time interval for adjacent curve is 10 min.

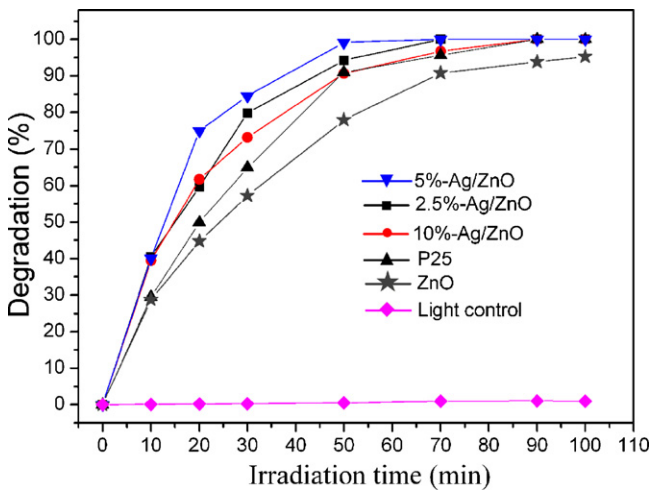

Fig. 7. Photodegradation curves of RhB by different catalysts.

perature. For samples S-400 and S-500, there are only very weak peaks at about 1500 and 3400 cm^{-1}, and some peaks observed in Fig. 5a almost disappear as shown in Fig. 5c and d. In addition, we found that, with the increase of calcination temperature, a new peak located at about 470 cm^{-1} emerged, contributing to the variation of Zn–O band of ZnO. For sample S-200, the peak cannot be observed, implying that no ZnO phase forms at this temperature (Fig. 5a). The peak becomes gradually strong with the increase of reaction temperature. For samples S-400 and S-500, very strong and obvious vibrations of Zn–O band are seen, implying the formation of ZnO. Temperature-dependent XRD and IR analyses indicate that the formation of Ag/ZnO should include several processes (the sequence in no order): (1) polymerization and carbonization of glucose under heat; (2) formation of Ag particles in glucose framework by the redox reaction of Ag^+ and glucose composition; (3) formation of ZnO particles; (4) the carbonized glucose gradually decompose under heat treatment, giving Ag/ZnO particles.

3.2. Photocatalyst test

The combination of Ag and ZnO are particularly interesting for photocatalytic application. In our study, the Ag/ZnO could be easily prepared with a high throughout, which should be favorable for their practical application. Organic dye RhB, a typical pollutant in the textile industry, has severe impact on the environment of relevance to our daily life. Thus, in our study, the photocatalytic performance of Ag/ZnO is evaluated by using RhB as a representative dye pollutant. With irradiation under UV light (365 nm), the characteristic absorption of RhB at $\lambda = 553$ nm decreases gradually, and finally disappears within 50 min in the presence of Ag/ZnO particles (Fig. 6). While in the absence of light or catalyst, the concentration of RhB has no obvious change for long time (Fig. 7). The results show that both light and catalyst are necessary for the effective photodegradation of RhB dye. To evaluate the photocatalytic activity of Ag/ZnO furtherly, the photocatalytic test in that the Degussa P25, a benchmark photocatalyst was used as catalyst is also performed. The degradation percentage of RhB is about 86% after irradiation for 50 min, and the total degradation of RhB by Degussa P25 is achieved for 90 min (Fig. 7). The result implies that the Ag/ZnO composite is a superior photocatalyst to Degussa P25 for photodegradation of the dye. However, the pure ZnO particles exhibit a lower activity than that of Degussa P25. The degradation percentage of RhB is about 76% after irradiation with UV light for 50 min in the presence of ZnO (Fig. 7). The RhB cannot be totally degradated by ZnO even for more than 100 min after photoirradiation. In addition, the Ag amount has an obvious effect on the photocatalytic performance of Ag/ZnO composites. The photodegradation percentage of RhB dye is about 92%, 100% and 86% for 2.5%-Ag/ZnO, 5%-Ag/ZnO and 10%-Ag/ZnO, respectively after irradiation for 50 min (Fig. 7). The total degradation time of dye is about 70 min and 90 min for 2.5%-Ag/ZnO and 10%-Ag/ZnO photocatalyst. The data was fitted based on pseudo-first order reaction kinetics $D = 100 \times [1 - \exp(-Kt)]$, as shown in Fig. 8. The apparent rate constant K was listed in Table 1. Based on the results, one can see that K value for all Ag/ZnO samples is higher than Degussa P25 and pure ZnO. The 5%-Ag/ZnO sample shows the highest catalytic activity with rate constant $K = 0.0954\ min^{-1}$ that is about 11 times higher than that of pure ZnO ($0.00859\ min^{-1}$) and 2 time than Degussa P25 (0.0469). These results show that the photocatalytic activity of ZnO can be obviously improved in the presence of Ag NPs. They also indicate that an appreciable amount of Ag is necessary to enhance the photocatalytic performance.

Table 1
The apparent rate constant K calculated for different catalyst systems.

Catalyst	ZnO	P25	2.5%Ag–ZnO	5%Ag–ZnO	10%Ag–ZnO
K (min^{-1})	0.00859	0.0469	0.0575	0.0954	0.0487

It is known that the activity of photocatalyst is relative to many factors, such as the size and the BET surface areas of materials. The BET surface for 2.5 wt%-Ag/ZnO, 5 wt%-Ag/ZnO and 10 wt%-Ag/ZnO is 2.1144, 2.7536, and 3.4775 m^2/g. For pure ZnO and Degussa P25, the BET surface area values are 10.2243 and 50 m^2/g, respectively. From these results, we found that: (1) the BET surface areas of all Ag/ZnO photocatalysts have similar values; (2) the pure ZnO and Degussa P25 have high surface area than Ag/ZnO composites. It is indicated that the high BET surface area are favorable for the improvement of the photocatalytic activity. Thus, the better performance of Ag/ZnO photocatalyst than P25 and ZnO particles is not due the BET factors, but is contributed the synergic action of Ag and ZnO particles. Zheng' et al. found that the optimized Ag content for Ag/ZnO catalyst is 5% (5.0-Ag/ZnO > 2.5-Ag/ZnO > ZnO; 5.0-Ag/ZnO > 10-Ag/ZnO > 20-Ag/ZnO) [35]. Lin et al. had studied photocatalytic performance Ag/ZnO heterostructured nanofibers prepared by electrospun methods and found that the activity of composites will be decreased when the Ag content exceeds 7.5%. The authors explained this by followed pointed: (1) the increase of Ag content will result in aggregation of Ag particles, thus the decrease of the number of active sites capturing the photoinduced electron; (2) excessive Ag can shield the UV light adsorption by ZnO,

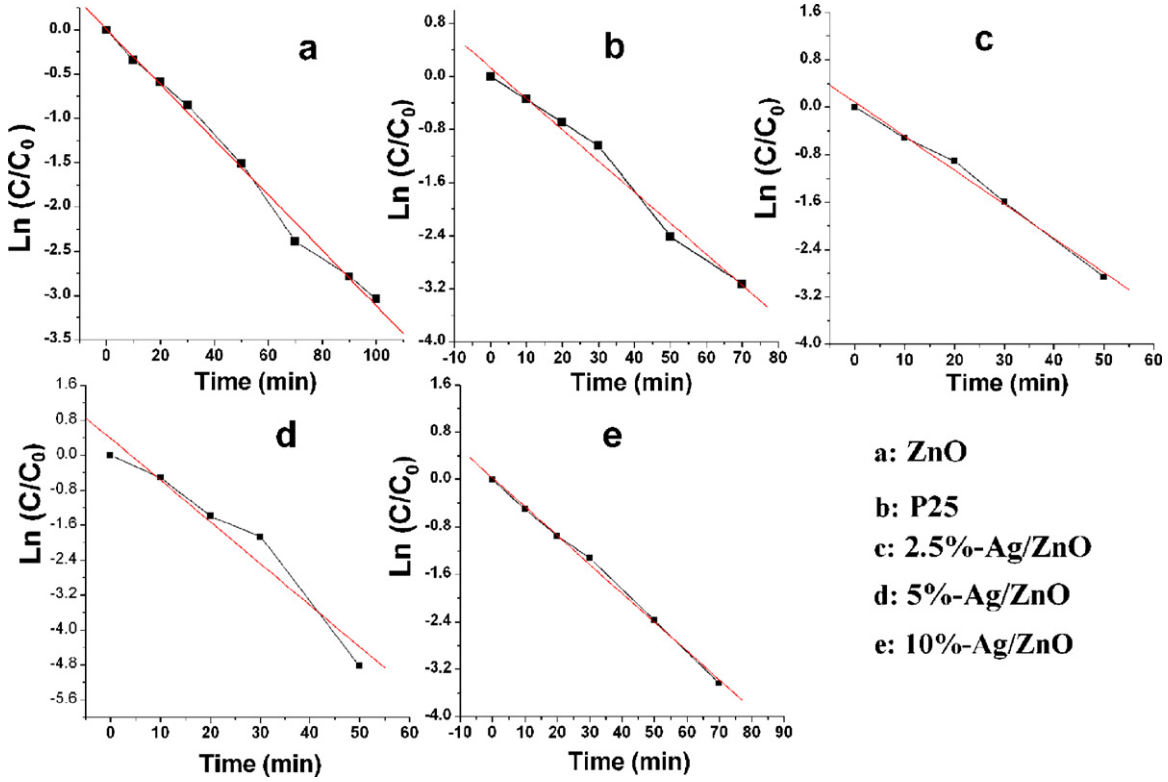

Fig. 8. $\ln(C/C_0)$ versus time curves of photodegradation of RhB. The C and C_0 are the reaction concentration and the initial concentration of RhB dye, respectively. The experimental data are fitted using the pseudo first-order kinetic equation: $\ln(C/C_0) = -Kt$.

deteriorating the photon utilizing efficiency. As an overall effect, the photocatalytic activity of the catalyst is therefore depressed [34]. Recently, we have also observed the enhanced photocatalyst activity and stability of Ag/ZnO composites compared to that of pure ZnO [38]. With appropriate ratio of Ag and ZnO, Ag/ZnO microspheres showed the better photocatalytic performance than commercial Degussa P25 TiO_2. PL and SPS studies indicated that the deposition of appropriate amount of Ag on ZnO surface is necessary to inhibit the recombination of photo induced electron–hole pairs. Present results about effect of Ag content on photocatalytic activity are consistent with previous reports [34,35,38]. Based on above analysis, the effect of Ag modification on the photocatalytic performance ZnO could be explained by followed points: (1) Ag NPs could inhibit the recombination of photoinduced carriers of ZnO, thus the photocatalytic performance of ZnO could be improved by Ag modification; (2) excessive Ag can shield the UV light adsorption of ZnO, thus decrease the photon utilizing efficiency. As results, the photocatalytic activity of the catalyst is therefore depressed as more Ag was used.

One of the major drawbacks of ZnO photocatalysts is their severe photocorrosion under UV irradiation [10,11], which can result in significant decrease of the photocatalytic activity in reused process. Some studies indicate that the photocatalytic activity of ZnO could be improved by tuning their texture, microstructure, but the recycled performance is still not satisfactory. Zhu et al. have found that modification of ZnO with polyaniline [41] and C60 [42] could improve notably the photostability of ZnO. Ours and Zheng's studies indicated that the stability of ZnO in photocatalytic process could be improved by Ag modification [35,38]. In the present work, the recycled performance of Ag/ZnO is also evaluated due to its importance for the practical application of photocatalysts. The irradiation time for each test is 50 min. As shown in Fig. 9, the photocatalytic efficiency of Ag/ZnO has no visible change even after ten recycles. The results indicated that Ag/ZnO photocatalyst has a good reuse performance. As control, the reuse performance of Degussa P25 was also investigated. As shown, the degradation efficiency of RhB is about 82% in five cycles for Degussa P25 catalyst, and 75% for ten cycles. The decrease in the photocatalytic efficiency of Degussa P25 should be related to the adsorption of organic molecules on the catalyst surface. Also, it is difficult to totally separate Degussa P25 from the system even with the assistance of high-speed centrifugation as its excellent dispersion in water. This leads to the loss of Degussa P25, and consequently, a decrease of its photocatalytic activity in recycled process. In contrast, the Ag/ZnO composites could easily settle down from a reaction system within 10 min, only with the assistance of low-speed centrifugation. This is beneficial

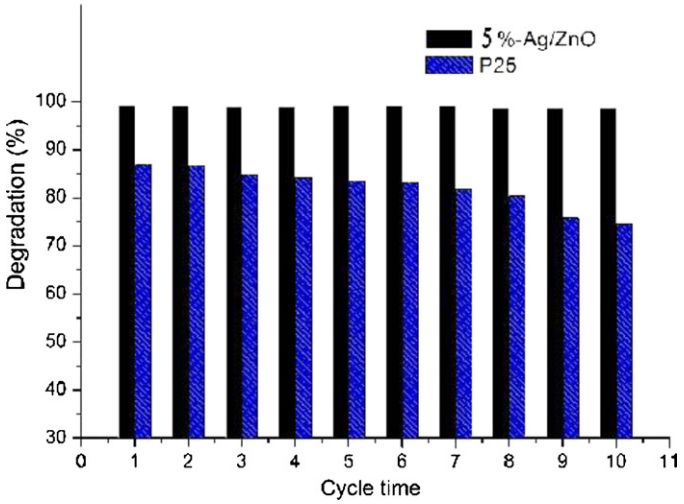

Fig. 9. Recycled performances of 5%-Ag/ZnO and Degussa P25 for photodegradation of RhB.

for the separation and reuse of catalysts. It is obvious that Ag/ZnO composites are suitable photocatalysts due to their high activity, good recycled performance accompanied by easy separation from reaction system. The enhanced photostability of Ag/ZnO catalyst is related to the Ag modification on the ZnO surface [35,38,43]. In addition, Ag/ZnO are prepared by calcination at higher temperature (600 °C), and thus the products have a high crystallinity, which also contributes to the high durability and activity of the materials [44,45].

4. Conclusions

The glucose-assisted "solution–solid" process is demonstrated to be effective way for preparing Ag/ZnO photocatalyst with a high yield. The products exhibited superior photocatalytic activity to unmodified ZnO and Degussa P25 TiO_2 for the photodegradation of RhB dye. Also, the Ag/ZnO catalysts have a good stability. After ten cycles, there is no obvious lost in photocatalytic activity. The enhanced photocatalytic performance of Ag/ZnO catalyst is related to the Ag modification on the ZnO surface and high crystallinity coming from the heat treatment at a high temperature. The proposed solution–solid route is facile, powerful, and high-throughput, thus providing a new approach for the development of high-performance ZnO-based photocatalysts.

Acknowledgements

We gratefully acknowledge the support of the Key Program Projects of the National Natural Science Foundation of China (no. 21031001), the National Natural Science Foundation of China (nos. 20971040, 21001042), the Cultivation Fund of the Key Scientific and Technical Innovation Project, Ministry of Education of China (no. 708029), the China Postdoctoral Science Foundation (no. 20080440919), Youth Foundation of Heilongjiang Province of China (QC2010021), the supporting plan for Excellent Youth of Common Universities of Heilongjiang province of China (no. 1154G24), the Scientific Research Fund of Heilongjiang Provincial Education Department (no. 11541283), Doctoral Research Foundation of Heilongjiang University and Youth Science Foundation of Heilongjiang University (QL200711).

Appendix A. Supplementary data

Supplementary data associated with this article can be found, in the online version, at doi:10.1016/j.jallcom.2011.04.005.

References

[1] M.N. Chong, B. Jin, C.W.K. Chow, C. Saint, Water Res. 44 (2010) 2997–3027.
[2] M.R. Hoffmann, S.T. Martin, W.Y. Choi, D.W. Bahnemann, Chem. Rev. 95 (1995) 69–96.
[3] X.L. Hu, G.S. Li, J.C. Yu, Langmuir 26 (2010) 3031–3039.
[4] D. Ravelli, D. Dondi, M. Fagnoni, A. Albini, Chem. Soc. Rev. 38 (2009) 1999–2011.
[5] A. Fujishima, K. Honda, Nature 238 (1972) 37–38.
[6] A.L. Linsebigler, G.Q. Lu, J.T. Yates, Chem. Rev. 95 (1995) 735–758.
[7] M.D. Hernández-Alonso, F. Fresno, S. Suárez, J.M. Coronado, Energy Environ. Sci. 2 (2009) 1231–1257.
[8] J.G. Yu, X.X. Yu, Environ. Sci. Technol. 42 (2008) 4902–4907.
[9] H.D. Muller, F. Steinbach, Nature 225 (1970) 728–729.
[10] A.J. Hoffman, E.R. Carraway, M.R. Hoffmann, Environ. Sci. Technol. 28 (1994) 776–785.
[11] A.V. Dijken, A.H. Janssen, M.H.P. Smitsmans, D. Vanmaekelbergh, A. Meijerink, Chem. Mater. 10 (1998) 3513–3522.
[12] G. Ramakrishna, H.N. Ghosh, Langmuir 19 (2003) 3006–3012.
[13] N. Kaneva, I. Stambolova, V. Blaskov, Y. Dimitriev, S. Vassilev, C. Dushkin, J. Alloys Compd. 500 (2010) 252–258.
[14] E.S. Jang, J.H. Won, S.J. Hwang, J.H. Choy, Adv. Mater. 18 (2006) 3309–3312.
[15] A. Mclaren, T. Valdes-Solis, G.Q. Li, S.C. Tsang, J. Am. Chem. Soc. 131 (2009) 12540–12541.
[16] M.S. Mohajerani, A. Lak, A. Simchi, J. Alloys Compd. 485 (2009) 616–620.
[17] X.J. Wang, Q.L. Zhang, Q. Wan, G.Z. Dai, C.J. Zhou, B.S. Zou, J. Phys. Chem. C 115 (2011) 2769–2775.
[18] H.B. Lu, S.M. Wang, L. Zhao, J.H. Li, B.H. Dong, Z.X. Xu, J. Mater. Chem. 21 (2011) 4228–4234.
[19] F. Lu, W.P. Cai, Y.G. Zhang, Adv. Funct. Mater. 18 (2008) 1047–1056.
[20] Y.N. Xia, Y.J. Xiong, B. Lim, S.E. Skrabalak, Angew. Chem. Int. Ed. 48 (2009) 60–103.
[21] V. Subramanian, E. Wolf, P.V. Kamat, J. Phys. Chem. B 105 (2001) 11439–11446.
[22] H. Zhang, G. Wang, D. Chen, X.J. Lv, J.H. Li, Chem. Mater. 20 (2008) 6543–6549.
[23] H. Zeng, P. Liu, W. Cai, S. Yang, X. Xu, J. Phys. Chem. C 112 (2008) 19620–19624.
[24] H.B. Zeng, W.P. Cai, P.S. Liu, X.X. Xu, H.J. Zhou, C. Klingshirn, H. Kalt, ACS Nano 2 (2008) 1661–1670.
[25] J. Yuan, E.S.G. Choo, X.S. Tang, Y. Sheng, J. Ding, J.M. Xue, Nanotechnology 21 (2010) 185606 (10 pp.).
[26] M.K. Lee, H.F. Tu, J. Electrochem. Soc. 155 (2008) D758–D762.
[27] Q. Wang, B.Y. Geng, S.Z. Wang, Environ. Sci. Technol. 43 (2009) 8968–8973.
[28] P. Pawinrat, O. Mekasuwandumrong, J. Panpranot, Catal. Commun. 10 (2009) 1380–1385.
[29] N. Morales-Flores, U.E. Pal, S. Mora, Appl. Catal. A: Gen. 394 (2011) 269–275.
[30] C. Pacholski, A. Kornowski, H. Weller, Angew. Chem. Int. Ed. 43 (2004) 4774–4777.
[31] L.Q. Jing, D.J. Wang, B.Q. Wang, S.D. Li, B.F. Xin, H.G. Fu, J.Z. Sun, J. Mol. Catal. A: Chem. 244 (2006) 193–200.
[32] C.D. Gu, C. Cheng, H.Y. Huang, T.L. Wong, N. Wang, T.Y. Zhang, Cryst. Growth Des. 9 (2009) 3278–3285.
[33] Y.H. Zheng, C.Q. Chen, Y.Y. Zhan, X.Y. Lin, Q. Zheng, K.M. Wei, J.F. Zhu, J. Phys. Chem. C 112 (2008) 10773–10777.
[34] D.D. Lin, H. Wu, R. Zhang, W. Pan, Chem. Mater. 21 (2009) 3479–3484.
[35] Y.H. Zheng, L.R. Zheng, Y.Y. Zhan, X.Y. Lin, Q. Zheng, K.M. Wei, Inorg. Chem. 46 (2007) 6980–6986.
[36] C. Karunakaran, V. Rajeswari, P. Gomathisankar, J. Alloys Compd. 508 (2010) 587–591.
[37] D.H. Zhang, X.H. Liu, X. Wang, J. Alloys Compd. 509 (2011) 4972–4977.
[38] C.G. Tian, W. Li, K. Pan, Q. Zhang, G.H. Tian, W. Zhou, H.G. Fu, J. Solid State Chem. 183 (2010) 2720–2725.
[39] X.M. Sun, Y.D. Li, Angew. Chem. Int. Ed. 43 (2004) 597–601.
[40] P. Raveendran, J. Fu, S.L. Wallen, J. Am. Chem. Soc. 125 (2003) 13940–13941.
[41] H. Zhang, R.L. Zong, Y.F. Zhu, J. Phys. Chem. C 113 (2009) 4605–4611.
[42] H.B. Fu, T.G. Xu, S.B. Zhu, Y.F. Zhu, Environ. Sci. Technol. 42 (2008) 8064–8069.
[43] W. Xie, Y.Z. Li, W. Sun, J.C. Huang, H. Xie, X.L. Zhao, J. Photochem. Photobiol. A 216 (2010) 149–155.
[44] H.L. Xu, W.Z. Wang, Angew. Chem. Int. Ed. 46 (2007) 1489–1492.
[45] G.H. Tian, H.G. Fu, L.Q. Jing, B.F. Xin, K. Pan, J. Phys. Chem. C 112 (2008) 3083–3089.